2004

Analysis of Structural Mistuning Effects on Bladed Disc Vibrations Including Aerodynamic Damping

Yoon S. Choi
Purdue University

Dana A. Gottfried
Purdue University

Sanford Fleeter
Purdue University

ANALYSIS OF STRUCTURAL MISTUNING EFFECTS ON BLADED DISC VIBRATIONS INCLUDING AERODYNAMIC DAMPING

Yoon S. CHOI, Dana A. GOTTFRIED, Sanford FLEETER

Purdue University, Department of Mechanical Engineering
West Lafayette, Indiana, USA
Phone: 765-494-5622, *Fax:* 765-494-0530, *E-mail:* fleeter@purdue.edu

ABSTRACT

A mathematical model is developed to investigate the effects of aerodynamic damping on the maximum amplification factor of mistuned bladed disks. LINSUB, an inviscid linearized unsteady aerodynamic damping code, provides unsteady aerodynamic damping influence coefficients, which are incorporated into a single-degree-of-freedom per blade mistuning model. The mistuning analysis including unsteady aerodynamic damping is then utilized to demonstrate the effect of aerodynamic damping on the maximum amplification factor of mistuned bladed disks. The relative importance of aerodynamic effects is determined by a comparison of an aerodynamic damping factor with the structural damping factor. Comparison of model results to data shows that including unsteady aerodynamic damping improves the prediction.

1. INTRODUCTION

1.1 Mistuning Overview

High Cycle Fatigue (HCF) of turbomachine blading resulting from flow-induced vibrations is a significant problem throughout the gas turbine industry. To address this problem, various approaches have been developed to predict airfoil resonant response. In these, the response of a tuned airfoil row, i.e. a rotor with all airfoils having the same structural properties and thus identical natural frequencies, is analyzed.

In fact, there are small airfoil-to-airfoil structural property variations that result, for example, from the manufacturing process or as a consequence of in-service wear. These are collectively referred to as mistuning and are known to lead to significant increases in airfoil resonant response amplitudes as compared to that of the tuned airfoil row, with mistuning thus often cited as a source of HCF in gas turbine engines. Hence, the key metric that characterizes the resonant response of mistuned bladed disks is the amplification factor (A.F.), the ratio of a blade's response amplitude on a mistuned bladed disk to its response amplitude on a tuned bladed disk.

Turbomachinery rotors typically have been bladed disks, with individual airfoils inserted into a slotted disk and retained by means of a dove-tail or fir-tree attachment. However, advances in manufacturing techniques have resulted in bladed-disk assemblies with increased uniformity, i.e. the blade-to-blade natural frequency variation, termed mistuning, is small. In addition, new design and manufacturing techniques have enabled the development and implementation of integrally bladed rotors (IBR's) wherein the blades and disk are machined from a single piece of material. IBR's have even less blade-to-blade mistuning than do bladed disks. Unfortunately, smaller mistuning does not translate into smaller amplification factors. On the contrary, as mistuning decreases the maximum amplification factor on a disk tends to increase until some threshold is reached at which point it decreases rapidly toward one. Figure 1 shows this trend as observed by Ottarsson and Pierre (1995) and Rivas-Guerra and Mignolet (2001) in numerical studies wherein many hundreds of bladed disks are simulated for each percent mistuning, with the maximum resulting A.F. taken. The decrease in mistuning due to new manufacturing methods is on the negative slope portion of Figure 1, thus rendering the new manufacturing methods a strong impetus for improving models which predict mistuned bladed disk response.

In contrast to the maximum A.F. of Figure 1, a theoretical maximum A.F. as derived by Whitehead (1966) does not depend on the size of the mistuning. The "Whitehead limit" for A.F. depends only on the number of blades N as $0.5\left(1+\sqrt{N}\right)$. Kenyon et al. (2003) have shown that if the phase shift of the forcing function from blade-to-blade is other than 0^o or 180^o, the maximum theoretical amplification factor is reduced to $0.5\left(1+\sqrt{N/2}\right)$. Taking

these theoretical maxima into account during design is an important first step in building blade rows resistant to HCF failure.

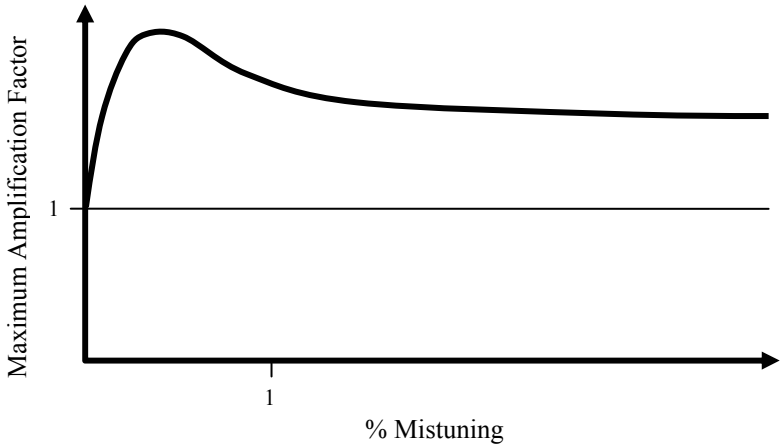

Figure 1. Amplification factor versus mistuning level.

Although an important first step, the above theoretical maxima need refinement under certain circumstances. First of all, the A.F. can be larger than the theoretical maximum for forcing frequencies and vibration mode shapes in the neighborhood of more than one mode family of the bladed disk (Kenyon, Griffin, Kim, 2003), i.e. in the neighborhood of veering regions. Second, the A.F. is often much less than the theoretical maximum which is based on several "worst case" assumptions. In an effort not to over-design for fatigue life and to gain insight into mistuned bladed disk behavior, refined mistuning models have been developed. These refined models resort to direct modeling of the bladed disk by distributed spring-mass systems or finite element analyses.

Lumped parameter models are the simplest of the refined mistuning models wherein the spring stiffnesses and masses are adjusted so that the dynamic characteristics of the model approximate that of the real bladed disk for the mode family or families of interest. Wei and Pierre (1988) and Rivas-Guerra and Mignolet (2003) among others use a lumped parameter model with one degree of freedom per blade to model one mode family. This approach has the advantage of simplicity and yields insights into general mistuning behavior. Kenyon, Griffin, and Kim (2003) have used three degrees of freedom per blade to model bladed disk dynamics in veering regions. In these lumped parameter models large numbers of mistuned bladed disks are simulated, with the resulting responses analyzed statistically, e.g. the probability that the maximum A.F. is larger than X is calculated.

Full finite element models of the bladed disk cannot be used for such deterministic/statistical approaches due to the large computational resources that would be required. Reduced order models keep some of the accuracy of full finite element models while improving on the accuracy of the lumped parameter models. Yang and Griffin (1997) developed a reduced order model based on finite element analyses of a tuned disk alone and a tuned blade alone. Yang and Griffin (2003) later developed a reduced order model that uses the modes of the tuned bladed disk to characterize the mistuned mode shapes, with this approach called "Subset of Nominal Modes" (SNM). Feiner and Griffin (2002) simplified the SNM model for the special case when a single mode family dominates the bladed disk response, with the simplicity of this model comparable to that of lumped parameter models. Like the lumped parameter models, all these reduced order models can simulate large numbers of mistuned bladed disks with the resulting responses analyzed statistically.

1.2 Aerodynamic Damping

These mistuning models consider the primary structural properties of the mistuned bladed disk. However, one significant phenomenon not addressed is the airfoil row unsteady aerodynamics. Since damping is known to be the important parameter controlling maximum resonant response amplitude, it might be expected that the unsteady aerodynamics resulting from the vibration of the blading itself, specifically the aerodynamic damping, will have a significant effect on the resonant response amplitude of tuned bladed disks as well as the A.F. of mistuned bladed disks. Note that the mechanical damping is considerably reduced in newer rotor designs, particularly those with integral bladed-rotors (IBR's) and those without shrouds. As a result, it is anticipated that aerodynamic damping will be particularly important in the vibratory stress analysis of mistuned IBR's.

Two families of techniques are utilized to predict aerodynamic damping of blade rows: time marching and time linearized. Time-marching techniques applied to the fluid equations, e.g. the potential, Euler, or Navier-Stokes equations, are the most widely used. However, this approach is computationally expensive, rendering them unsuitable for use in simulations directed at determining the maximum A.F. of a mistuned bladed disk.

In time-linearized analyses, the fluid equations are linearized by considering the flow unsteadiness to be small compared to the mean flow. The resulting small disturbance equations are then solved assuming that the disturbance flow is harmonic in time with a constant interblade phase angle between adjacent blades. The advantage of time-linearized models is that they are computationally very efficient as compared to the time-marching approach. Thus, they are well-suited for use in mistuning simulations. In this regard, LINSUB (Whitehead, 1987) is a widely used and generally available inviscid linearized unsteady aerodynamic code.

Unfortunately, the basic assumptions inherent in both time-marching and linearized unsteady aerodynamic damping analyses are too restrictive for mistuning simulations. Specifically, the airfoils are required to oscillate harmonically with uniform amplitude and a constant phase relationship or interblade phase angle between airfoils. However, if there are airfoil-to-airfoil material differences, i.e. mistuning, the mistuned airfoils respond in patterns that are inconsistent with the assumptions of uniform vibration amplitude and interblade phase angle.

This paper is directed at investigating the effects of aerodynamic damping on the amplification factor of mistuned bladed disks. First, the restrictions of uniform blade vibration amplitude and constant interblade phase angle are removed. This is accomplished by utilizing an inverse transform technique to determine the influence coefficients that characterize the unsteady aerodynamic influence of each individual airfoil oscillating with its own unique amplitude. With the aerodynamic damping of each airfoil on the row thus determined, this unsteady aerodynamic damping influence coefficient analysis is incorporated into a lumped parameter mistuning model with one degree of freedom per blade. The simplicity of the lump parameter equations of motion allows the relative importance of the aerodynamic damping to be determined by a comparison of a structural damping coefficient and an unsteady aerodynamic damping coefficient.

2. UNSTEADY AERODYNAMIC MODEL

LINSUB is a linearized, semi-analytic unsteady aerodynamic model for turbomachinery geometries. The model simplifies the turbomachinery airfoil row to a two-dimensional cascade of thin airfoils with the flow unsteadiness assumed a small perturbation from the uniform steady flow. A wide range of unsteady flow phenomena are modeled including cascade vibrations in an otherwise uniform flow which are of interest herein. The predicted unsteady pressure distribution on the airfoils is integrated to obtain the lift, moment, or chordwise bending force on each airfoil. LINSUB assumes a complex harmonic time dependence of $e^{i\omega t}$, resulting in complex unsteady aerodynamic coefficients that allow for differing phase between the airfoil vibration and unsteady aerodynamic force.

2.1 Removing Interblade Phase Angle Restriction

Yoon, Gottfried, and Fleeter (2003) describe how the LINSUB coefficients are transformed into influence coefficients, which have no interblade phase angle restriction. The complex influence coefficient $\widehat{C}_j^k$ is the generalized unsteady aerodynamic force acting on Airfoil j due to a unit amplitude motion of Airfoil k with all other airfoils stationary. Thus, for example, the unsteady aerodynamic moment on Airfoil 4 due to vibration of Airfoil 2 with amplitude α_2 is $\widehat{C}_4^2\,\alpha_2 e^{i\omega t}$, where the real part is taken to obtain the physically measurable moment.

3. MATHEMATICAL MODEL

The mistuned bladed disk forced response model including aerodynamic damping effects is depicted in Figure 2. Note that k_c models the stiffness of the disk which couples airfoil to airfoil, k_j is the stiffness of airfoil j, and $\overline{c}$ is the structural damping of each airfoil. The unsteady aerodynamic damping ζ^{aero} is the imaginary part of the unsteady aerodynamic loading.

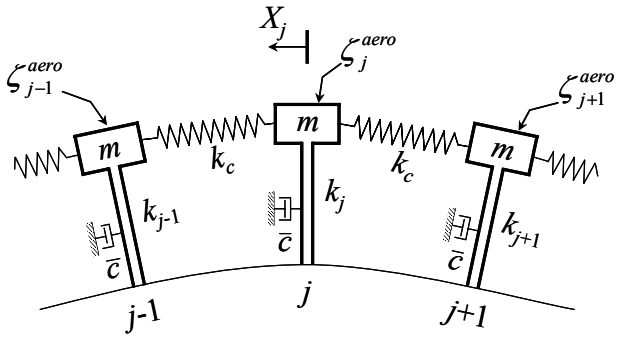

Figure 2. Airfoil row single-degree-of-freedom model

The dimensional equation of motion for Airfoil j is

$$m\ddot{X}_j + \bar{c}\dot{X}_j + \left(k_j + 2k_c\right)X_j - k_c X_{j-1} - k_c X_{j+1} = F_j\left(t\right) + L_j \tag{1}$$

where $F_j(t)$ is the forcing function generated by the wake or potential field from adjacent airfoil rows, X_j is the generalized displacement of Airfoil j, and L_j is the sum total of aerodynamic forces on Airfoil j due to the vibration of each airfoil in the row.

Equation 1 applies to a two-dimensional slice through the airfoil row and models any single-degree-of-freedom mode such as bending, torsion or chordwise bending. For example, if torsion is modeled, m is the moment-of-inertia, L_j is the aerodynamic moment, $F_j(t)$ is the forcing function specified in terms of time varying moment, and X_j is the angular displacement of Airfoil j.

The generalized aerodynamic force depends on the single-degree-of-freedom mode being considered.

Bending

$$L_j = \sum_{k=0}^{N-1}\left[\hat{C}_j^k\right]^L \rho u\, c\dot{X}_k$$

Torsion

$$L_j = \sum_{k=0}^{N-1}\left[\hat{C}_j^k\right]^M \rho u^2\, c^2 X_k$$

Chordwise Bending

$$L_j = \sum_{k=0}^{N-1}\left[\hat{C}_j^k\right]^{CW} \rho u^2 c^2 X_k \tag{2}$$

where the superscript L on the influence coefficient means lift-due-to-bending, the superscript M means moment-due-to-torsion and the superscript CW denotes chordwise bending, the density and relative speed of the air flow are ρ and u, the airfoil chord length is c, and the number of airfoils around the annulus is N.

The forcing function can be decomposed into spatial and temporal harmonics, with each harmonic analyzed separately in this linear system. Thus consider a harmonic forcing function

$$F_j(t) = F_0 e^{i\left(\omega t + (j-1)\,\beta_R\right)} \qquad j = 1, 2, \ldots, N \tag{3}$$

where β_R is the "interblade phase angle" or phase difference from one airfoil to the next, and F_0 is the forcing function amplitude. Due to circular symmetry β_R is restricted to the values $2\pi R/N$, where R is any integer between 0 and N-1, inclusive.

The generalized displacement is assumed to have the form $X_j(t) = x_j e^{i\omega t}$, $j = 1, 2, \ldots, N$. Thus the equation of motion in matrix form is

$$\begin{bmatrix} \hat{D}_1^1 & -\left(k_c + \Gamma_1^2\right) & -\Gamma_1^3 & \cdots & -\left(k_c + \Gamma_1^N\right) \\ -\left(k_c + \Gamma_2^1\right) & \hat{D}_2^2 & -\left(k_c + \Gamma_2^3\right) & \cdots & -\Gamma_2^N \\ -\Gamma_3^1 & -\left(k_c + \Gamma_3^2\right) & \hat{D}_3^3 & \cdots & -\Gamma_3^N \\ \vdots & \vdots & \vdots & \ddots & \vdots \\ -\left(k_c + \Gamma_N^1\right) & -\Gamma_N^2 & -\Gamma_N^3 & \cdots & \hat{D}_N^N \end{bmatrix} \begin{Bmatrix} x_1 \\ x_2 \\ x_3 \\ \vdots \\ x_N \end{Bmatrix} = \begin{Bmatrix} F_0 \\ F_0 e^{i\beta_R} \\ F_0 e^{i2\beta_R} \\ \vdots \\ F_0 e^{i(N-1)\beta_R} \end{Bmatrix} \tag{4}$$

where the Γ's are the aerodynamic terms: $\Gamma_j^k = i\omega\rho uc\left[\hat{C}_j^k\right]^L$ for bending, $\Gamma_j^k = \rho u^2 c^2\left[\hat{C}_j^k\right]^M$ for torsion, and $\Gamma_j^k = \rho u^2 c^2\left[\hat{C}_j^k\right]^{CW}$ for chordwise bending. The diagonal term is $\hat{D}_j^j = -m\omega^2 + i\omega\overline{c} + k_j + 2k_c - \Gamma_j^j$.

Solving the linear system of Equation 4 for a given set of airfoil stiffnesses k_j and aerodynamic and structural conditions yields the mistuned response of the system including unsteady aerodynamic effects.

4. COMPARISON OF STRUCTURAL & UNSTEADY AERODYNAMIC DAMPING

The importance of aerodynamic effects relative to structural effects is ascertained by examination of Equation 4. The structural damping is the imaginary term $i\omega\overline{c}$ on the diagonal. Aerodynamic damping results from the imaginary part of Γ_j^k and is present in every term in the coefficient matrix. However, the diagonal Γ , i.e. Γ_j^j, is the aerodynamic force on an airfoil due to its own motion, with this term much larger than the off-diagonal Γ's. Thus, a comparison of $\omega\overline{c}$ and $\mathrm{Im}\left(\Gamma_j^j\right)$ is a comparison of the relative importance of structural damping and aerodynamic damping. In terms of the nondimensional damping parameter, these two quantities are

$$\zeta^{mech} = \frac{\overline{c}}{2m\omega} \qquad \zeta^{aero} = -\frac{\mathrm{Im}\left(\Gamma_j^j\right)}{2m\omega^2} \tag{5}$$

If $\zeta^{mech} >> \zeta^{aero}$, aerodynamic damping has little effect, while if $\zeta^{mech} \approx \zeta^{aero}$, aerodynamic damping will have a noticeable effect.

5. RESULTS

The mistuning analysis including unsteady aerodynamic effects is applied to the IBR of the Purdue transonic axial compressor. This compressor has an 8.0 in. I.D., a 12.0 in. O.D., with 20 Inlet Guide Vanes (IGV's) 18 rotor blades and 20 stators. With this IGV/blade count the forcing to the blades has interblade phase angle $\beta_R = 2\pi(2)/18$.

The Campbell diagram of Figure 3 shows the modal natural frequencies versus rotor RPM for mode shapes having interblade phase angle 2π(2)/18.. The 20 upstream IGVs excite the rotor at 20 times the engine RPM, with this excitation frequency indicated by the 20E line. This 20E line crosses the fourth mode at approximately 17,000 RPM, with this resonant crossing closest to the design speed of 20,000 RPM. Thus, in the following analysis an operating point at this resonant crossing is considered.

Since the majority of the energy transfer from the flow field to the blade typically occurs near the blade tip, the airfoil section at 90% span is taken as the representative section in the mistuning model. Among the three mode shapes to choose from in the mistuning model, i.e. bending, torsion, or chordwise bending, an ANSYS model of the fourth mode shows that at 90% span bending most closely approximates the mode.

IBR's have less damping than conventional bladed disks with blades mechanically attached to the disk. Thus the damping coefficient is set to 0.001, a damping coefficient lower than that of conventional bladed disks.

A summary of the structural and aerodynamic properties of this IBR model is given in Table 1.

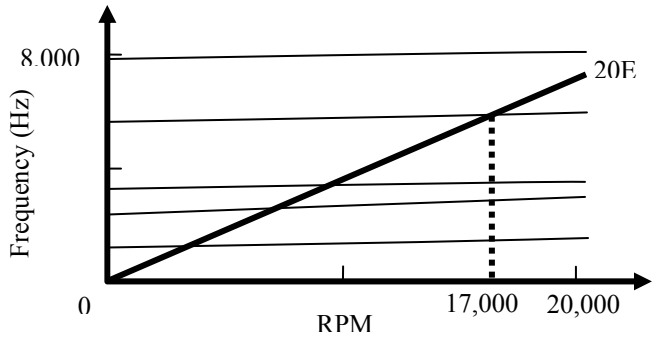

Figure 3. Campbell diagram for modes with interblade phase angle 2π(2)/18.

Table 1. IBR structural and aerodynamic properties

Properties Required for Structural Part of Model	
Inertia, m	0.5948 kg/m
Structural stiffness, k_t	6.48×10^8 N/m^2
Structural damping, ζ^{mech}	0.001
Structural coupling, k_c	$0.377k_t$
Properties Required for Unsteady Aero Part of Model	
SDOF mode (for aero only)	bending
Spacing-to-chord ratio	1.018
Stagger from axial	64.72°
Mach number, w_o/a	0.84
Reduced frequency, $\omega c/w_o$	6.36
Chord, c	0.05 m
Span	0.05 m
Stagnation properties	STP

With the rotor off the shaft, the stiffness of each blade was measured experimentally with the result shown in Figure 4 in terms of the mistuned stiffness $\delta k_j = k_j - k_t$ normalized by k_t, where k_t is the average stiffness of all the blades. The deviation of frequency from the average frequency, i.e. $\delta\omega_j/\omega_t$, is approximately $0.5\delta k_j/k_t$, so the maximum frequency deviation is -4.4% for blade 18. The root-mean-square of $\delta\omega_j/\omega_t$ is 1.9%.

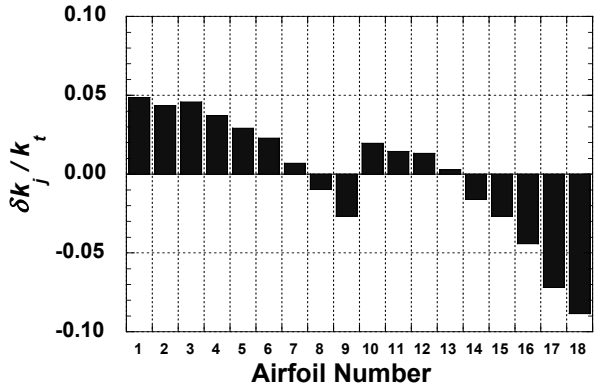

Figure 4. Airfoil mistuning stiffness pattern

To show the importance of including unsteady aerodynamics in resonant response mistuning models and hence the need for the mistuning model developed herein, the response of the IBR at the fourth mode resonant crossing is analyzed. Upon evaluating the unsteady aerodynamic influence coefficients and using Equation 5, it is determined that the unsteady aerodynamic damping is equal to the structural damping, i.e. $\zeta^{mech} = 0.001 = \zeta^{aero}$. Hence it is expected that the unsteady aerodynamics will have a significant effect.

A tuned analysis reveals that without unsteady aerodynamics, the ratio of bending vibration amplitude to forcing amplitude is $7.12\text{x}10^{-7}$ m/(N/m), while with unsteady aerodynamics the same ratio is $3.97\text{x}10^{-7}$ m/(N/m), about half as large due to the additional unsteady aerodynamic-based damping.

The amplification factor versus frequency for the 20E excitation with and without unsteady aerodynamics is shown in Figure 5. The frequency is normalized by ω_2, the natural frequency of the fourth mode at $ND = 2$. A bold line represents the tuned normalized amplitude, with the 18 thin lines representing the A.F. of all 18 blades.

In contrast to the tuned solution, the mistuned results have several peaks in the frequency range 0.92 to 1.08, a consequence of the distortion of mode shapes caused by mistuning. For a tuned airfoil row, the 20E excitation is orthogonal to all mode shapes except the 2 *ND* mode shape. Thus, only one peak appears. With mistuning, the natural mode shapes are distorted and the 20E excitation has non-zero projections onto these mode shapes. As a result, all modes contribute to the response at their respective natural frequencies. The two peaks near $\omega/\omega_2 = 1.0$

are from the perturbed forward traveling 2 *ND* mode shape and the perturbed backward traveling 2 *ND* mode shape, both of which have natural frequencies close to 1.0.

For the mistuned rotor, Airfoil 4 has the peak response amplitude with and without unsteady aerodynamics. The amplification factor for Airfoil 4 is 1.0813 at $\omega/\omega_2 = 0.997$ without unsteady aerodynamics and 0.9461 at $\omega/\omega_2 = 0.997$ with unsteady aerodynamics. Thus, mistuning has resulted in increased response amplitude without unsteady aerodynamics but a decreased amplitude with unsteady aerodynamics.

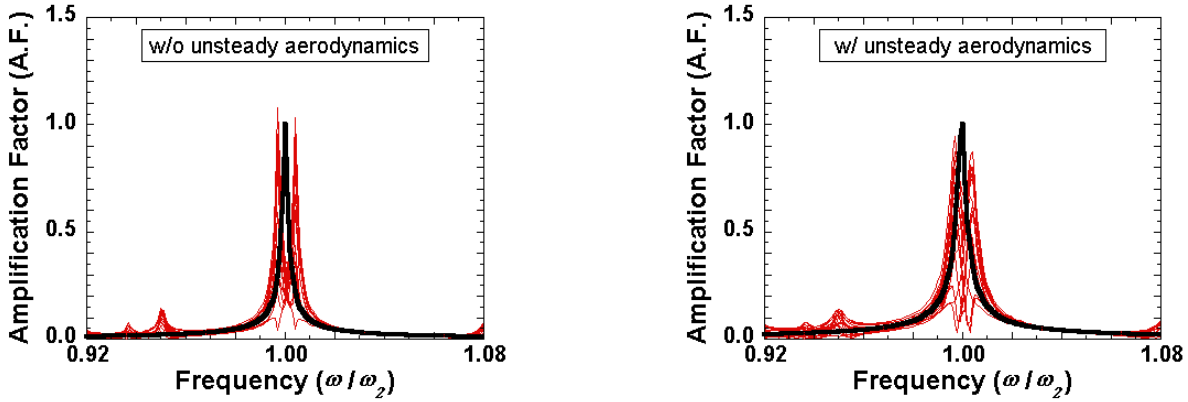

Figure 6. Amplification factor versus excitation frequency, without and with unsteady aerodynamics.

A noninterference stress-measurement system was used to experimentally measure vibratory amplitudes for the rotor operating at the 17,000 rpm resonant crossing at nominal loading (Fulayter, 2004). Since the tuned amplitude is not experimentally available, the vibration amplitudes are normalized by the average vibration amplitude of all the blades, with this normalized amplitude plotted as the solid bars in Figure 7. Also shown in Figure 7 are the predicted response amplitudes with and without unsteady aerodynamics, with each prediction normalized by its average response amplitude. Both the data and predictions correspond to the frequency at which response was maximized, which for the models occurs at $\omega/\omega_2 = 0.997$. Since the location of Airfoil 1 in Figure 4 was not tracked, the data of Figure 7 was shifted so that the maximum for both data and prediction occurs at the same blade, Blade 4.

Both the data and predictions in Figure 7 have similar character, with four peaks around the rotor. The models largely under-predict the amplitude for several blades, e.g. blades 1, 11 and 15. However, the most important metric, the maximum normalized amplitude, has a difference of less than 0.1 between data and prediction.

The maximum normalized amplitude is 1.73 for the model without unsteady aerodynamics, 1.68 for the model with unsteady aerodynamics, and 1.64 for the data. Thus including unsteady aerodynamic damping improves the predicted maximum response. In addition, the root-mean-square of the difference between model and data is 0.503 without unsteady aerodynamics and 0.488 with unsteady aerodynamics. Thus on a more global scale, including unsteady aerodynamics slightly improves the prediction.

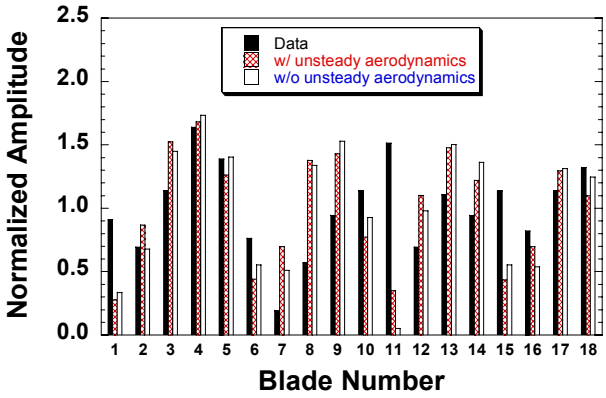

Figure 7. Response amplitude for each blade normalized by mean amplitude of all blades.

6. SUMMARY AND CONCLUSIONS

Unsteady aerodynamic damping is a significant contributor to the overall damping of bladed disks, especially as modern bladed disks follow a trend toward lower structural damping. It has been shown that unsteady aerodynamic damping can be incorporated into a mistuning analysis by use of coefficients from a linearized, semi-analytic unsteady aerodynamic model. Numerical studies based on the geometry and flow conditions of the Purdue IBR show that including aerodynamic damping has a significant effect on the predicted amplification factors. Comparison of model results to data shows that including unsteady aerodynamic effects improves the prediction.

REFERENCES

Choi, Y.S., Gottfried, D.A., Fleeter, S., 2003, Resonant Response of Mistuned Bladed Disks Including Aerodynamic Damping Effects, *AIAA Paper* AIAA-2003-4977.

Feiner, D.M., Griffin, J.H., 2002, A Fundamental Model of Mistuning for a Single Family of Modes, *Journal of Turbomachinery*, vol. 124, no. 4, p. 597-605.

Fulayter, R., 2004, An Experimental Investigation of Resonant Response of Mistuned Fan and Compressor Rotors Utilizing NSMS, *Purdue University*, Department of Mechanical Engineering, Ph.D. Thesis.

Kenyon, J.A., Griffin, J.H., Feiner, D.M., 2003, Maximum Bladed Disk Forced Response From Distortion of a Structural Mode, *Journal of Turbomachinery*, vol. 125, no. 2: p. 352-363.

Kenyon, J.A., Griffin, J.H., Kim, N.E., 2003, Frequency Veering Effects on Mistuned Bladed Disk Forced Response, *39th AIAA/ASME/SAE/ASEE Joint Propulsion Conference and Exhibit*, AIAA paper 2003-4976.

Ottarsson, G., Pierre, C., 1995, On the Effects of Interblade Coupling on the Statistics of Maximum Forced Response Amplitudes in Mistuned Bladed Disks, *AIAA/ASME/ASCE/AHS/ASC Structures, Structural Dynamics & Materials Conference*, no. 5: p 3070-3078.

Rivas-Guerra, A.J., Mignolet, M.P., 2001, Local/Global Effects of Mistuning on the Forced Response of Bladed Disks, *Proc. ASME Turbo Expo*, 2001-GT-0289: p. 1-11.

Rivas-Guerra, A.J., Mignolet, M.P., 2003, Maximum amplification of blade response due to mistuning: Localization and mode shape aspects of the worst disks, *Journal of Turbomachinery*, vol. 125, no. 3: p. 442-454.

Wei, S.T., Pierre, S., 1988, Localization Phenomena in Mistuned Assemblies with Cyclic Symmetry Part 1: Free Vibrations, Journal of Vibration, Acoustics, Stress, and Reliability in Design, vol. 110, no. 4: p. 439-449.

Whitehead, D.S., 1966, "Effect of Mistuning on the Vibration of Turbomachine Blades Induced by Wakes," *Journal of Mechanical Engineering Science*, Vol. 8, No. 1, p: 15-21.

Whitehead, D. S., 1987, Unsteady Two-Dimensional Linearized Subsonic Flow in Cascades, Chapter 3, *In:* Platzer, M.F., Carta, F.O., *AGARD Manual on Aeroelasticity in Axial-Flow Turbomachines, Volume 1, Unsteady Turbomachinery Aerodynamics*, AGARD-AG-298, p. 3-24 to 3-30.

Yang, M.-T., Griffin, J.H., 1997, A Reduced Order Approach for the Vibration of Mistuned Bladed Disk Assemblies, *Journal of Engineering for Gas Turbines and Power*, vol. 119, no. 1: p. 161-167.

Yang, M.-T., Griffin, J.H., 2003, A Reduced-Order Model of Mistuning Using a Subset of Nominal System Modes, *Journal of Engineering for Gas Turbines and Power*, vol. 123, no. 4: p. 893-900.